Simplified patterning process for the selective 1D ZnO nanorods growth

Simplified patterning process for the selective 1D ZnO nanorods growth

Yulin Geng, Karina Jeronimo, Muhammad Ammar Bin Che Mahzan, Peter Lomax, Enrico Mastropaolo, and Rebecca Cheung

Citation: Journal of Vacuum Science & Technology B **38**, 012204 (2020); doi: 10.1116/1.5131363
View online: https://doi.org/10.1116/1.5131363
View Table of Contents: https://avs.scitation.org/toc/jvb/38/1
Published by the American Vacuum Society

JVST B
Journal of Vacuum Science & Technology B

ARTICLE

avs.scitation.org/journal/jvb

Simplified patterning process for the selective 1D ZnO nanorods growth

Cite as: J. Vac. Sci. Technol. B 38, 012204 (2020); doi: 10.1116/1.5131363
Submitted: 11 October 2019 · Accepted: 17 December 2019 ·
Published Online: 30 December 2019

Yulin Geng,[a] Karina Jeronimo, Muhammad Ammar Bin Che Mahzan, Peter Lomax, Enrico Mastropaolo,[b] and Rebecca Cheung

AFFILIATIONS

Institute for Integrated Micro and Nano Systems, School of Engineering, University of Edinburgh, Scottish Microelectronics Centre, EH9 3FF Edinburgh, United Kingdom

Note: This paper is part of the Conference Collection: The 63rd International Conference on Electron, Ion, and Photon Beam Technology and Nanofabrication (EIPBN 2019).

[a]**Electronic mail:** Yulin.Geng@ed.ac.uk
[b]Deceased 15 July 2019.

ABSTRACT

A novel patterning method for the selective growth of ZnO nanorods has been developed, which can avoid any etching steps and longtime lift-off processes. In the simplified process, the deposition of a titanium buffer layer is omitted, and a 50 nm ZnO thin-film seed layer is deposited by e-beam evaporation directly onto the silicon patterned with the photoresist. The omitted titanium buffer layer has been observed to result in the absence of the ZnO seed layer on the photoresist. Then, the ZnO nanorods with diameters ranging from 50 to 500 nm have been found to grow hydrothermally only on the regions without the photoresist. The photoresist remains on the substrate after the hydrothermal growth, which can protect areas from the polluted solution and unwanted nanorods. After all processes, the photoresist can be removed easily by the solvent without any unwanted damage of nanorods. With this simplified method, ZnO nanorods can be synthesized and patterned with only one step of lithography, which can be used for novel ZnO based devices.

I. INTRODUCTION

Recently, zinc oxide (ZnO) nanostructures have received much attention due to their excellent performance in solar cells,[1,2] light emitting diodes,[3] photocatalysts,[4,5] chemical sensors,[6,7] field effect transistors,[8] and piezoelectric devices.[9–12] Until now, various methods have been developed to synthesize ZnO nanorods (NRs) such as wet chemical methods,[13,14] physical vapor deposition,[15,16] metal-organic chemical vapor deposition,[17] and top-down approaches by etching.[18] Among the various synthesis methods for ZnO NRs, the low-temperature hydrothermal growth method has drawn much attention and has been applied in low-cost nanofabrication processes.[14] Generally, before the hydrothermal growth, a seed layer is required to buffer the lattice mismatch between the ZnO NRs and substrates, and then ZnO NRs can grow hydrothermally with different morphologies on different substrates through the control of growth environments such as *p*H, growth time, precursor concentration, and temperature.[19–22] Combined with lithographic technology, ZnO NRs have been synthesized hydrothermally on various low dimensional nanomaterials, such as graphene[23,24] and MoS_2,[25] and have been developed to fabricate novel integrated microsystems with unique properties. However, the patterning and assembling steps of the 1D NRs to a specific region of the substrate materials are relatively complicated, which may include extra etching[26] or the longtime lift-off processes of the patterned ZnO NRs.[27] Currently, the most common method to pattern ZnO NRs is the lift-off process. There are two strategies used in lift-off patterning processes: lift-off NRs (Ref. 27) or lift-off the seed layer.[28,29] At least two steps of lithography are required to pattern, the ZnO NR-seed layer needs to be patterned first, and then an area of NRs growth needs to be defined by a second lithographic step, which may increase the complexity and cost during the fabrication process.

In our work, we introduce a new fabrication process that allows the selective growth of ZnO NRs with only one lithography

step, which can avoid any etching steps and lift-off processes. We have observed that electron beam (e-beam) evaporated ZnO seed layer stays on the patterned silicon (Si) when no titanium (Ti) buffer layer has been deposited before the ZnO seed layer evaporation. In other words, the ZnO seed layer has been observed to be absent on photoresist (PR) but forms on Si if the Ti buffer layer is omitted. Therefore, ZnO NRs can be synthesized selectively by the hydrothermal method onto patterned Si. The ZnO seed layer and NRs synthesized by this simplified method (no Ti buffer layer) have been analyzed and compared with the ZnO seed layer and NRs synthesized by conventional NRs lift-off methods (with the Ti buffer layer). Elemental analysis and morphology analysis have been performed on the seed layer and NRs to study the influence of the Ti buffer layer on the selective growth nature of NRs.

II. EXPERIMENTAL DETAILS

A. Sample preparation and lithography

Figure 1 shows the overall schematic process flow to pattern ZnO NRs on substrates; both current NR lift-off processes and our simplified method have been presented. Firstly, 3-in. silicon (Si) wafers have been chosen as the substrates [Fig. 1(a)]. Acetone, isopropyl alcohol (IPA), and de-ionized (DI) water, and oxygen (O_2) plasma ashing have been used to clean the substrates. Before the spin-coating of PR, substrates have been primed with hexamethyldisilazane (HMDS) vapor for 10 min to increase the adhesion of PR.

During the experiments, both positive resist SPR350 series and negative resist AZ nLOF 2070 series have been used in the lithography processes [Fig. 1(b)]. For instance, diluted (1:0.55) AZ2070 PR has been spin-coated with 4000 rpm to form resist films with a thickness of around 1.5 μm. After soft-baking at 100 °C for 1.5 min, the PR has been exposed by either a mask-aligner or a maskless direct-write machine. Different PR features have been patterned in our experiment. Next, postexposure baking has been performed on samples at 110 °C for 1 min and then developed in the MF26A or AZ developer for 1.5 min. Lastly, samples have been treated by 115 °C hard-baking to increase the stability of PR.

B. Pre-evaporation treatments: O_2 plasma and Ti buffer layer

The main difference between the current NRs lift-off processes and our simplified patterning methods is the pre-evaporation treatment [Fig. 1(c)]. Normally, before the deposition of thin-films, 3–5 min O_2 plasma ashing is used to treat the sample surface and clean the PR residues, and in some specific cases, the O_2 plasma treatment is reported to modify the wettability of the surface and improve the bonding between the as-deposited layer and the substrate.[30–32] In addition, an intermediate Ti or chromium (Cr) buffer layer is usually deposited to improve the adhesion of the ZnO thin-film seed layer to the substrate.[33,34] During our experiment, the influence of O_2 plasma and Ti buffer layer on the existence of the as-deposited ZnO seed layer and NRs has been investigated by four groups of samples: (a) treated with O_2 plasma and predeposited 10 nm Ti buffer layer; (b) treated with only O_2 plasma; (c) predeposited 10 nm Ti buffer layer only; and (d) no treatment.

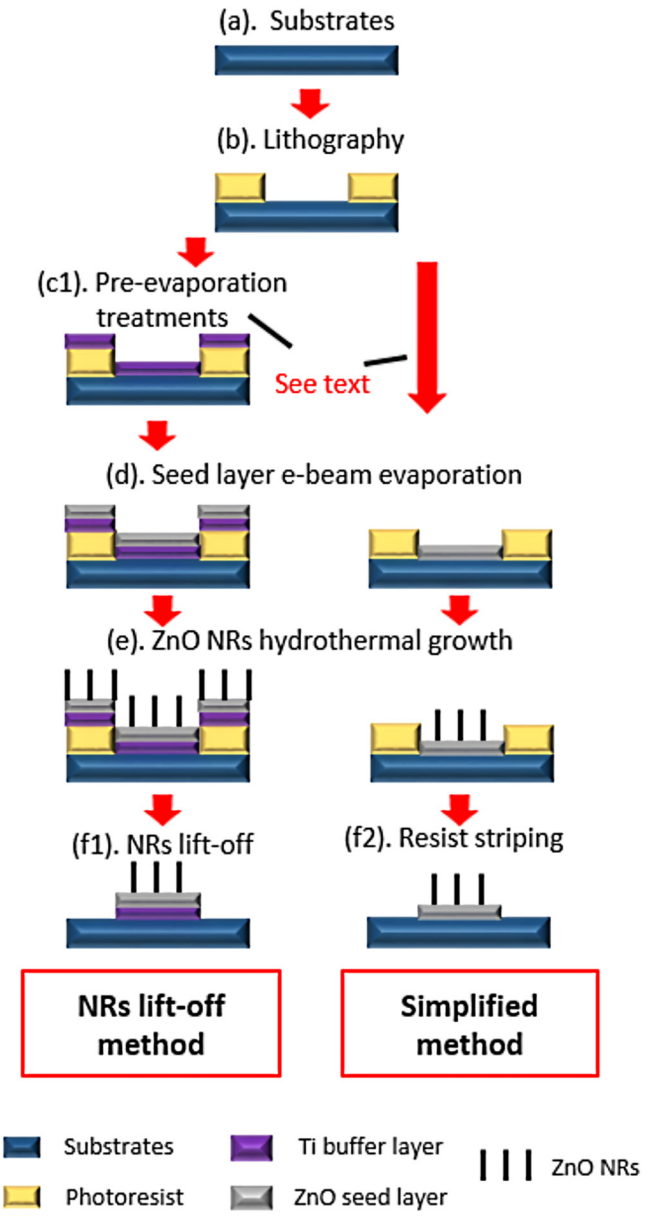

FIG. 1. Schematic of the simplified method on patterning ZnO NRs, as compared with the NRs lift-off method.

C. ZnO seed layer e-beam evaporation and NRs hydrothermal growth

ZnO seed layer thin-films with a thickness of 50 nm have been evaporated on all samples [Fig. 1(d)]. The ZnO target has been used as the evaporation source, the start vacuum pressure has been set at 2×10^{-6} torr, and the e-beam voltage has been fixed at 10 kV with ~3% output power, which can result in ZnO thin-film to be deposited at around 1 Å/s.

After the evaporation of ZnO seed layer thin-films, all the samples have been put top-side down and floated in 250 ml DI water with 40 mM 1:1 zinc nitrate hexahydrate [$Zn(NO_3)_2 \cdot 6H_2O$] and HMTA (hexamethylenetetramine) precursors. Then, ZnO NRs have been grown on samples at 90 °C for 18 h [Fig. 1(e)]. Once the hydrothermal process has been completed, lift-off [Fig. 1(f1)] or PR stripping [Fig. 1(f2)] can be performed with acetone or NMP1165 remover after characterization.

D. Characterization

The diameter and density of NRs have been investigated by scanning electron microscopy (SEM). Energy-dispersive x-ray spectroscopy (EDS) has been used to analyze the element of ZnO seed layers and ZnO NRs on both substrate (Si) and PR. The morphology of the ZnO seed layer has been investigated by atomic force microscopy (AFM).

III. RESULTS AND DISCUSSION

A. Influence of treatments before seed layer evaporation

The influence of O_2 plasma and Ti buffer layer on the existence of the as-deposited ZnO seed layer and NRs has been investigated on four groups of samples: (a) treated with O_2 plasma and predeposited 10 nm Ti buffer layer; (b) treated with only O_2 plasma; (c) predeposited 10 nm Ti buffer layer only; and (d) no treatment. The SEM images of ZnO NRs grown on four groups of samples have been shown in Fig. 2.

As shown in Figs. 2(b) and 2(d), no relationship between the existence of ZnO NRs and O_2 plasma has been observed since the O_2 plasma is expected only to clean PR residues. However, 10 nm Ti buffer layer has been found to be essential to the existence of the ZnO NRs. It has been observed that after hydrothermal growth, ZnO NRs with a diameter ranging from 60 to 250 nm distribute uniformly both in the region of Si and PR [Fig. 2(c)] with the ZnO seed layer on the Ti buffer layer. In contrast, without the Ti buffer layer, the ZnO NRs have been found to be almost absent on the PR, which is probably due to the poor bonding between the ZnO seed layer and PR. However, ZnO NRs have been observed to grow on the Si part of the sample with a diameter of around 300 nm, even without the Ti buffer layer [Fig. 2(d)].

To investigate the mechanism of the selective growth of ZnO NRs on patterned Si further, we focus on the influence of Ti buffer layer since O_2 plasma has not found to contribute to the existence of ZnO NRs on PR. The ZnO seed layer and NRs on the sample with Ti [sample (c)] or without Ti buffer layer [sample (d)] have been analyzed by EDS and AFM, which will be presented in Secs. III B–III C.

B. Elemental analysis on ZnO seed layer and ZnO NRs

EDS has been performed on the e-beam evaporated ZnO thin-film seed layer and ZnO NRs separately on both sample (c) with Ti and sample (d) without the Ti buffer layer. The percentage of elements has been presented in Table I. The penetration depth of the x ray has been fixed at around 1.5 μm by adjusting the beam density, and the detection areas have been fixed at 10 μm^2. Carbon and Si have also been detected as the main element of samples. However, these two elements are related to the PR contamination and Si substrates; thus, the data for C and Si have been omitted in Table I.

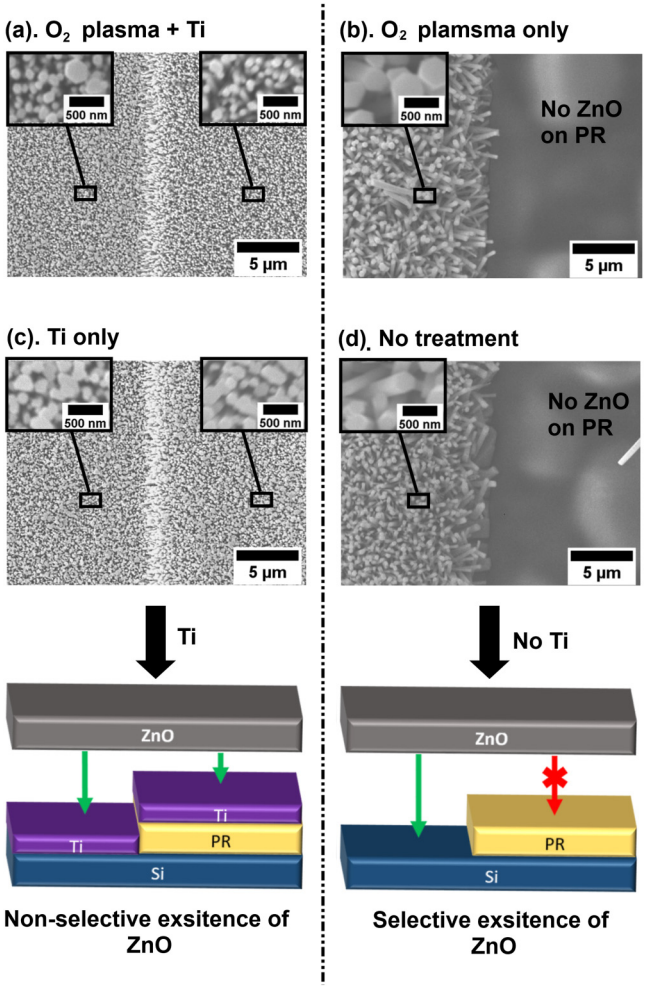

FIG. 2. SEM images of ZnO NRs grown on the samples with pre-evaporation treatment before ZnO seed layer deposition: (a) treated with O_2 plasma and predeposited 10 nm Ti buffer layer; (b) treated with only O_2 plasma; (c) predeposited 10 nm Ti buffer layer only, and (d) no treatment.

TABLE I. EDS analysis (element percentage) on a 50 nm e-beam evaporated ZnO seed layer and ZnO NRs grown by the hydrothermal method.

		ZnO seed layer			ZnO NRs	
Sample	Region	Ti	O	Zn	O	Zn
(c) With Ti	PR + Ti	0.27	8.4	0.32	39	36
	Si + Ti	0.66	2.4	0.84	47	49
(d) Without Ti	PR	0	5.0	0	3.9	0
	Si	0	0.4	0.04	42	54

As can be seen in Table I, for sample (c) with the Ti buffer layer, Zn element has been detected on the seed layer of both PR + Ti and Si + Ti regions, and after NRs growth, Zn and O have been observed to be the main elements on both PR + Ti and Si + Ti regions. As for sample (d) without the Ti buffer layer, no Zn has been detected on PR at all, neither after seed layer evaporation nor after NRs hydrothermal growth. However, a very low amount of Zn (0.04%) has been detected on the as-evaporated seed layer on the Si part. Then, Zn and O have been observed to become the main elements on the Si part after hydrothermal growth.

The results of elemental analysis in Table I indicate that the selective growth of ZnO NRs is due to the selective existence of ZnO seed layer on patterned Si without the Ti buffer layer. A Ti buffer layer can contribute to the existence of ZnO seed layer both on PR and on Si, which is probably because Ti can be oxidized naturally, and it can bond easily to other materials by the O dangling bonds.[35,36] Therefore, in our cases, the different layers probably bond in the form of Si/PR-O-Ti-O-Zn-O. However, without Ti, no bond or only weak bond can be formed between the ZnO seed layer and PR during the e-beam evaporation, which results in the absence of the ZnO seed layer on PR. The frequently reported weak adhesion of polymer and ZnO thin-films deposited by sputtering[20,34] might be another proof of the weak bond or even lack of bond between ZnO and PR. As for the Si part, some other researchers have reported that Si can naturally bond with ZnO directly in the form of Si-O-Zn-O,[37,38] which might be the reason for the existence of ZnO on Si without Ti.

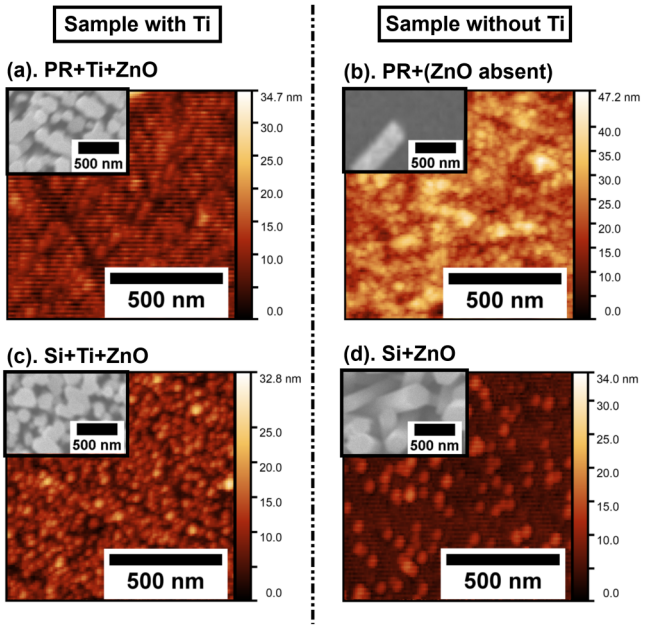

FIG. 3. AFM images on the ZnO seed layer with SEM images of as-grown ZnO NRs (90 °C, 18 h, 40 mM precursors concentration) inserted, the sample with the Ti buffer layer: (a) on PR and (c) on Si; the sample without Ti: (b) on PR and (d) on Si.

C. Morphology of patterned ZnO seed layer and structure of as-grown NRs

AFM has been performed to study the morphology of the ZnO seed layer by e-beam evaporation, and SEM has been used to study the diameter and density of the as-grown ZnO NRs on the seed layers. Figure 3 shows the images obtained by AFM and SEM, and Table II lists the surface properties of the seed layers as well as the diameter and density of as-grown NRs collected from AFM and SEM images.

For the sample with the Ti buffer layer, similar grain density and roughness of the ZnO seed layer on both PR + Ti [Fig. 3(a)] and Si + Ti [Fig. 3(c)] can be observed. Then, the ZnO NRs grown on both PR + Ti and Si + Ti have been found to have a similar diameter of ~140 nm and a similar density of ~34 NRs/μm^2 on both Si and PR regions. This observation indicates the "buffer" effect of the Ti layer, which results in a similar surface morphology of the ZnO seed layer on PR and Si, and therefore similar diameter and density of ZnO NRs.

On the other hand, for the sample without the Ti buffer layer, a really rough surface with irregular grains has been observed on the PR part of the sample after the seed layer evaporation [Fig. 3(b)], which corroborates with previous EDS results [sample (d) PR] of the absence of the ZnO seed layer on PR. Thus, only NRs debris can be seen on the PR after NRs' growth. However, on the Si part of sample (d) without Ti, it can be seen in Fig. 3(d) that the seed layer has a larger grain diameter but smaller grain density and roughness than the Si part of the sample with Ti [Fig. 3(c)]. Then after NRs' growth, ZnO NRs are observed to have a larger diameter and smaller density compared to the sample with Ti.

D. Microfabrication and future applications

Figure 4 shows the example results of patterning of 1D ZnO with the simplified method. Through our simplified method, the placement of the ZnO NRs can be precisely controlled to the selected area without any longtime lift-off process, and only one lithography step is required. As can be seen in Figs. 4(a) and 4(b),

TABLE II. Surface morphology of the as-evaporated ZnO seed layer collected from AFM images, together with the diameter and density of as-grown ZnO NRs collected from SEM images. The density is approximate value, with around ±10% errors, except from sample (d) PR region, the grain size is not well detected, and approximate value has been listed.

	ZnO seed layer			ZnO NRs	
	Grain diameter (nm)	Grain density (No./μm^2)	Roughness (nm)	Diameter (nm)	Density (No./μm^2)
PR + Ti	38	296	1.9	136	33.8
Si + Ti	32	308	2.1	144	33.5
PR	65 (approx.)	164 (approx.)	3.1	Absent	Debris
Si	40	92	1.6	210	11.5

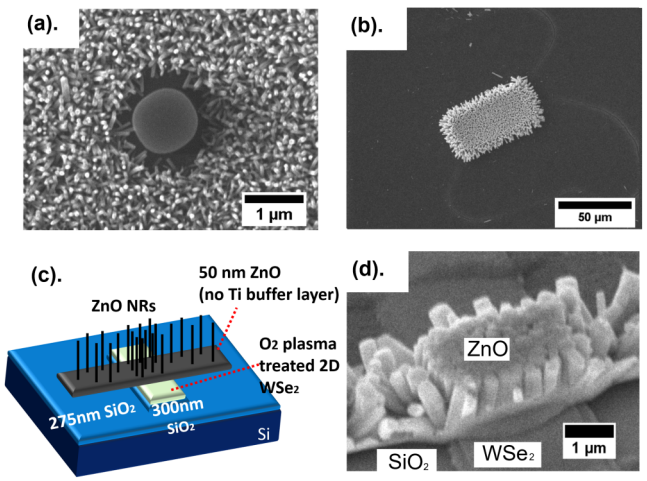

FIG. 4. Different patterned geometry with the simplified method: (a) patterned area (ZnO ≫ PR) and (b) patterned area (PR ≫ ZnO). Integration of 1D ZnO and 2D WSe_2 by the simplified method: (c) structure and (d) SEM image.

our simplified method is independent of patterned feature design, the placement of ZnO NRs can be achieved in both the case of area ratio PR ≫ Si and the case of Si ≫ PR. The reason is that the patterned geometry is not related to the mechanism of the absence of the ZnO seed layer on PR. However, the patterned geometry of PR will influence the mass transport during hydrothermal growth and thus affect the growth geometry of ZnO NRs,[29,39] which needs to be considered during the device design if the specific length, diameter, and density of NRs are required.

Apart from the Si substrate, without the Ti buffer layer, the selective growth of NRs has also be observed on SiO_2, aluminum (Al), silver (Ag), and even O_2 plasma-treated few-layer tungsten diselenide (WSe_2). For instance, Figs. 4(c) and 4(d) show the integration of 1D ZnO NRs and 2D few-layer WSe_2 by this simplified method. WSe_2 has been prepared by mechanical exfoliation and treated with O_2 plasma. Then, the simplified method has been used to grow ZnO NRs on the specific area of 2D WSe_2. As can be seen in Fig. 4(d), well vertical-aligned and very dense ZnO NRs have been grown on the top of WSe_2. In addition, the adhesion of patterned ZnO NRs to the substrate has been examined by putting samples in the ultrasonic bath. ZnO NRs produced by our simplified method can survive for longer than 10 min, which suggests the possibility of our simplified method to pattern ZnO NRs for piezoelectric sensing or nanogenerating applications. Moreover, this method opens up possibilities to integrate ZnO NRs with other low dimensional materials, and the heterostructure may be used for future applications in novel strain/stress sensor, biomimetic skin, or nanorobots.

IV. SUMMARY AND CONCLUSIONS

In summary, we have studied the influence of pre-evaporation treatments (O_2 plasma and the Ti buffer layer) on the selective existence of the e-beam evaporated ZnO seed layer on patterned Si. The hydrothermal growth of the ZnO NRs on the selectively present ZnO seed layer has been studied. The O_2 plasma has not been found to influence the selective existence of the ZnO seed layer, while Ti buffer has been found to play an important role in the existence of the ZnO seed layer. With the Ti buffer layer, ZnO seed layer stays on both Si and PR, and then ZnO NRs have been observed to grow with a uniform density of ~34 NRs/μm^2 and similar diameters of 140 nm on both Si and PR parts. While without the Ti buffer layer, the ZnO seed layer has been found to be absent on PR but stay on Si; thus, ZnO NRs have been seen to grow on Si part only, with a less density of ~11 NRs/μm^2 and a larger diameter of ~210 nm than the sample with the Ti buffer layer. Our simplified method for patterning ZnO NRs is inspired by the selective existence of the ZnO seed layer on PR patterned Si when the Ti buffer layer is omitted. Compared with the current NRs patterning process (with Ti), our simplified method requires only one lithography step to control the location of the ZnO NRs precisely without any longtime lift-off or etching steps, which is suitable in the fabrication of future piezoelectric sensors or nanogenerators.

ACKNOWLEDGMENTS

The authors acknowledge the financial support of the UK Engineering and Physical Sciences Research Council (EPSRC) for this work. The China Scholarship Council (CSC) is acknowledged for financial support through the Ph.D. scholarship at the University of Edinburgh. The work was performed in the Scottish Microelectronics Centre and Institute for Integrated Micro and Nano Systems, University of Edinburgh. The authors would like to thank Stewart Ramsay for the e-beam evaporation processes.

REFERENCES

[1]R. Vittal and K. C. Ho, Renew. Sustain. Energy Rev. **70**, 920 (2017).
[2]V. Manthina and A. G. Agrios, Superlattices Microstruct. **104**, 374 (2017).
[3]X. M. Zhang, M. Y. Lu, Y. Zhang, L. J. Chen, and Z. L. Wang, Adv. Mater. **21**, 2767 (2009).
[4]X. Zhang, J. Qin, Y. Xue, P. Yu, B. Zhang, L. Wang, and R. Liu, Sci. Rep. **4**, 4596 (2014).
[5]S. Baruah, M. Jaisai, R. Imani, M. M. Nazhad, and J. Dutta, Sci. Technol. Adv. Mater. **11**, 05002 (2010).
[6]R. Kumar, O. Al-Dossary, G. Kumar, and A. Umar, Nanomicro Lett. **7**, 97 (2015).
[7]L. Zhu and W. Zeng, Sens. Actuators A **267**, 242 (2017).
[8]Y. W. Heo, L. C. Tien, Y. Kwon, D. P. Norton, S. J. Pearton, B. S. Kang, and F. Ren, Appl. Phys. Lett. **85**, 2274 (2004).
[9]Z. L. Wang, Adv. Funct. Mater. **18**, 3553 (2008).
[10]Z. L. Wang, Adv. Mater. **19**, 889 (2007).
[11]J. Briscoe and S. Dunn, Nano Energy **14**, 15 (2014).
[12]Y. Zhang, Y. Liu, and Z. L. Wang, Adv. Mater. **23**, 3004 (2011).
[13]R. A. Laudise and A. A. Ballman, J. Phys. Chem. **64**, 688 (1960).
[14]L. Vayssieres, Adv. Mater. **15**, 464 (2003).
[15]M. H. Huang, Y. Wu, H. Feick, N. Tran, E. Weber, and P. Yang, Adv. Mater. **13**, 113 (2001).
[16]B. D. Yao, Y. F. Chan, and N. Wang, Appl. Phys. Lett. **81**, 757 (2002).
[17]W. Il Park, G. C. Yi, M. Kim, and S. J. Pennycook, Adv. Mater. **14**, 1841 (2002).
[18]J. J. Wu, H. I. Wen, C. H. Tseng, and S. C. Liu, Adv. Funct. Mater. **14**, 806 (2004).
[19]Z. L. Wang, Mater. Sci. Eng. R Rep. **64**, 33 (2009).

[20]S. Xu and Z. L. Wang, Nano Res. **4**, 1013 (2011).
[21]G. Amin, M. H. Asif, A. Zainelabdin, S. Zaman, O. Nur, and M. Willander, J. Nanomater. **2011**, 269692 (2011).
[22]V. Manthina and A. G. Agrios, Nano-Struct. Nano-Objects **7**, 1 (2016).
[23]G.-H. Nam, S.-H. Baek, C.-H. Cho, and I.-K. Park, Nanoscale **6**, 11653 (2014).
[24]V. Quang Dang, D.-I. Kim, L. Thai Duy, B.-Y. Kim, B.-U. Hwang, M. Jang, K.-S. Shin, S.-W. Kim, and N.-E. Lee, Nanoscale **6**, 15144 (2014).
[25]L. Chen, F. Xue, X. Li, X. Huang, L. Wang, J. Kou, and Z. L. Wang, ACS Nano **10**, 1546 (2016).
[26]R. Shi, C. Huang, L. Zhang, A. Amini, K. Liu, Y. Shi, S. Bao, N. Wang, and C. Cheng, Sci. Rep. **6**, 1 (2016).
[27]A. Syed, M. Kalloudis, V. Koutsos, and E. Mastropaolo, Microelectron. Eng. **145**, 86 (2015).
[28]J. Song, S. Baek, H. Lee, and S. Lim, J. Nanosci. Nanotechnol. **9**, 3909 (2009).
[29]M. Maddah, C. P. Unsworth, and N. O. V. Plank, Mater. Res. Express **6**, 015905 (2019).
[30]D. Wojcieszak, A. Poniedziałek, M. Mazur, J. Domaradzki, D. Kaczmarek, and J. Dora, Mater. Sci. Pol. **34**, 418 (2016).
[31]K. C. Tang, E. Liao, W. L. Ong, J. D. S. Wong, A. Agarwal, R. Nagarajan, and L. Yobas, J. Phys. Conf. Ser. **34**, 155 (2006).
[32]M. Yamamoto, T. Matsumae, Y. Kurashima, H. Takagi, T. Suga, T. Itoh, and E. Higurashi, Micromachines **10**, 119 (2019).
[33]S. Xu, Y. Wei, J. Liu, R. Yang, and Z. L. Wang, Nano Lett. **8**, 4027 (2008).
[34]S. Xu, Y. Wei, M. Kirkham, J. Liu, W. Mai, D. Davidovic, R. L. Snyder, and L. W. Zhong, J. Am. Chem. Soc. **130**, 14958 (2008).
[35]A. M. Chaze and C. Coddet, Oxid. Met. **28**, 61 (1987).
[36]M. Todeschini, A. Bastos Da Silva Fanta, F. Jensen, J. B. Wagner, and A. Han, ACS Appl. Mater. Interfaces **9**, 37374 (2017).
[37]Z. Shen, H. Zhou, H. Chen, H. Xu, C. Feng, and X. Zhou, Nanomaterials **8**, 317 (2018).
[38]Y. Chen, H. Ding, and S. Sun, Nanomaterials **7**, 217 (2017).
[39]J. M. Lee, Y.-S. No, S. Kim, H.-G. Park, and W. Il Park, Nat. Commun. **6**, 6325 (2015).